Semicond. Sci. Technol. **26** (2011) 055019 (5pp) doi:10.1088/0268-1242/26/5/055019

Accurate measurement of the formation rate of iron–boron pairs in silicon

J Tan, D Macdonald, F Rougieux and A Cuevas

School of Engineering, College of Engineering and Computer Science, The Australian National University, Canberra, 0200 ACT, Australia

E-mail: jason.tan@anu.edu.au

Received 4 November 2010, in final form 20 January 2011
Published 23 March 2011
Online at stacks.iop.org/SST/26/055019

Abstract

This paper presents new data regarding the formation rate of iron–boron (Fe_i–B) pairs in p-type crystalline silicon. Improvements in the temperature control of the sample, a reduction in measurement error of the effective lifetime of the sample after all Fe_i–B pairs have reformed, and improved statistical analysis have led to a revision of the value of the pre-factor in the equation relating the association time constant of iron–acceptor pairs to the acceptor concentration. The new equation predicts a 14% slower repairing time than a previous commonly used equation, and reduces the uncertainty in determining the acceptor concentration from the repairing time from ±24% to ±7%.

(Some figures in this article are in colour only in the electronic version)

1. Introduction

Most studies of compensated silicon require knowledge of the acceptor dopant concentration (N_A). One of the simplest techniques to determine N_A in p-type silicon is via the reformation of dissociated iron–boron pairs (Fe_i–B) [1]. This technique is proving to be a useful tool in studies of compensated silicon [2–4].

However, recent measurements of Fe_i–B association time constants (τ_{assoc}) utilizing a temperature-controlled WCT-100 Sinton Consulting instrument [5] have indicated that the pre-factor in the equation published by Macdonald *et al* [6] (5×10^5 cm^{-3} K^{-1}) requires some adjustment. In addition, the original measurements were accurate to ±3 K. If we only consider the error in temperature, the ±3 K translates to an uncertainty of ±24% for N_A based on this equation.

In this paper, we present Fe_i–B repairing data acquired in a more rigorous manner, comprising much better temperature control and a more thorough statistical analysis of the results. This leads to a significantly lower uncertainty when using the iron–acceptor pairing technique for determining acceptor concentrations in p-type silicon.

2. Experimental details

P-type silicon samples of various resistivities were etched in a 10:1 HNO_3/HF solution to a thickness of ∼200 μm and chemically cleaned. Fe^{56} was implanted into one surface of the samples with an energy of 70 keV, and a dose of 5×10^{10} cm^{-2}. The Fe was then evenly distributed throughout the wafer thickness, by a 900 °C 1 h anneal in a nitrogen atmosphere. The samples were lightly etched again before RCA cleaning and passivation of both surfaces with plasma-enhanced chemical vapour deposited amorphous silicon nitride. After optically dissociating the Fe_i–B pairs, the changing effective lifetime of the samples was characterized at 35 °C ± 0.2 °C using the temperature-controlled WCT-100 described by Paudyal *et al* [7]. The effective lifetime of the samples was sampled at an excess carrier density (Δn) of 1×10^{15} cm^{-3}. Only the minimum flash intensity required to reach $\Delta n = 1 \times 10^{15}$ cm^{-3} was used during data acquisition, to minimize separation of Fe_i–B pairs. Six to seven data points were fitted to extract τ_{assoc}. These points corresponded to 0–85% of the interstitial Fe population having repaired with a B atom. The exclusion of effective lifetime data points corresponding to 85–100% reformation of the Fe_i–B population helped minimize the impact of experimental noise on the extracted τ_{assoc}.

In order to calculate the N_A of the samples, the conductance of the samples was measured using a carefully calibrated inductive coil (see section 3.3). N_A was calculated from the conductance of the sample (σ), the sample thickness

(W), the hole mobility (μ_p), and the electron charge (q) using the equation

$$NA = \frac{\sigma}{\mu_p q W}.$$

The hole mobility was derived from the Klaassen [8, 9] mobility model. Other mobility models were considered [10, 11]; however, the difference between the models in the doping range of interest was only ~2%.

3. Experimental uncertainties

Four parameters directly influence the accuracy of the experiment. In order of importance, they are

(1) sample temperature stability during Fe_i–B pair reformation,
(2) the accuracy of the final repaired effective lifetime (τ_{final}),
(3) calibration of the inductive coil used to determine σ and hence N_A of the samples, and
(4) ensuring complete randomization of dissociated Fe through the silicon lattice.

The mitigation of the uncertainties associated with each of these parameters will be discussed below.

3.1. Minimizing temperature errors

Although the temperature of the sample stage in the modified WCT-100 is actively controlled by PID switching [7], it was prudent to check the temperature uniformity across the inductive coil, as well as the long-term stability of the stage temperature. To do this, four 0.003 in diameter k-type thermocouples were attached to a silicon wafer using conductive silver paste. This structure was placed over the inductive coil once the temperature-controlled stage had reached 35.0 °C. The thermocouples were connected to a Pico USB TC-08 data logger sampling at 1 Hz [12]. The sample temperature within the area measured by the inductive coil was very uniform and well within 35 °C ± 0.2 °C. Figure 1 demonstrates the temperature stability of the stage over extended periods. From this figure we can see that the sample temperature is well within the target of 35 °C ± 0.2 °C.

3.2. Minimizing τ_{final} errors

The effective lifetime corresponding to full repairing of the Fe_i–B population (τ_{final}) has a strong impact on the accuracy of the τ_{assoc} derived from the fit of the data. To minimize experimental noise, at least ten measurements of τ_{final} were taken (as shown in the tail of the curves displayed in figure 2) and averaged. Each measurement was spaced at intervals long enough to ensure full repairing of any Fe_i–B pairs broken by the flash used to acquire effective lifetime data. The standard deviation of the τ_{final} data was between 0.5% and 2%.

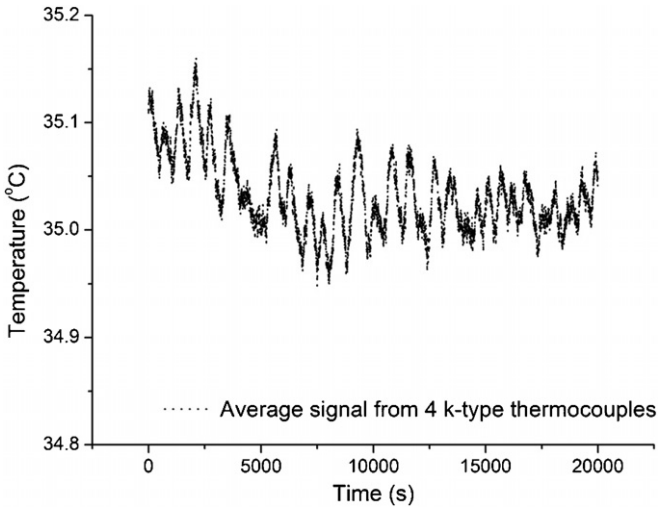

Figure 1. The stability of stage temperature over extended periods of time.

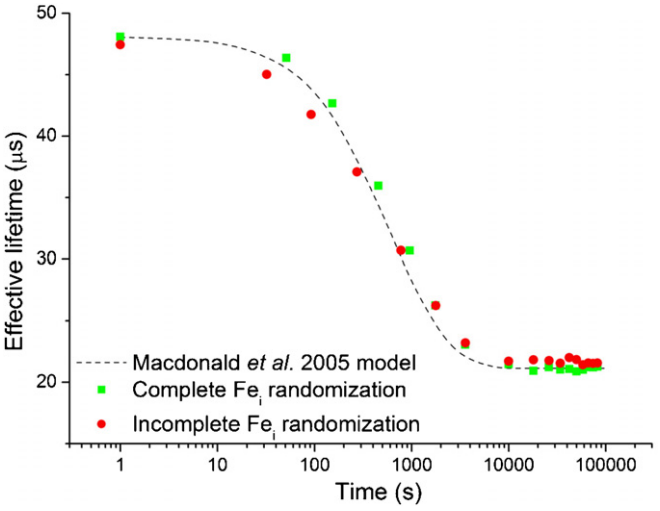

Figure 2. Two Fe_i–B repairing curves measured from the same sample.

3.3. Minimizing coil calibration errors

Although the τ_{assoc} measurements were carried out with the temperature-controlled WCT-100 [7], a standard WCT-120 [13] instrument was used to determine the conductance and hence N_A of the samples. This inconsistency was justified by the fact that the modified WCT-100 inductive coil is less sensitive than the standard WCT-120 inductive coil, due to its smaller coil diameter and the metallic heating stage which surrounds the coil. Low sensitivity in the 1–10 mS range would have a strong impact on several of the samples used in this experiment. Although the stage temperature of the WCT-120 is not as well controlled as the modified WCT-100, the ~0.5 °C temperature variation detected during the calibration of the coil and subsequent measurement of the samples has almost no impact on the samples' conductance and hence their corresponding N_A.

Six phosphorus diffused wafers and nine non-diffused wafers were used to calibrate the inductive coil. The resistivity

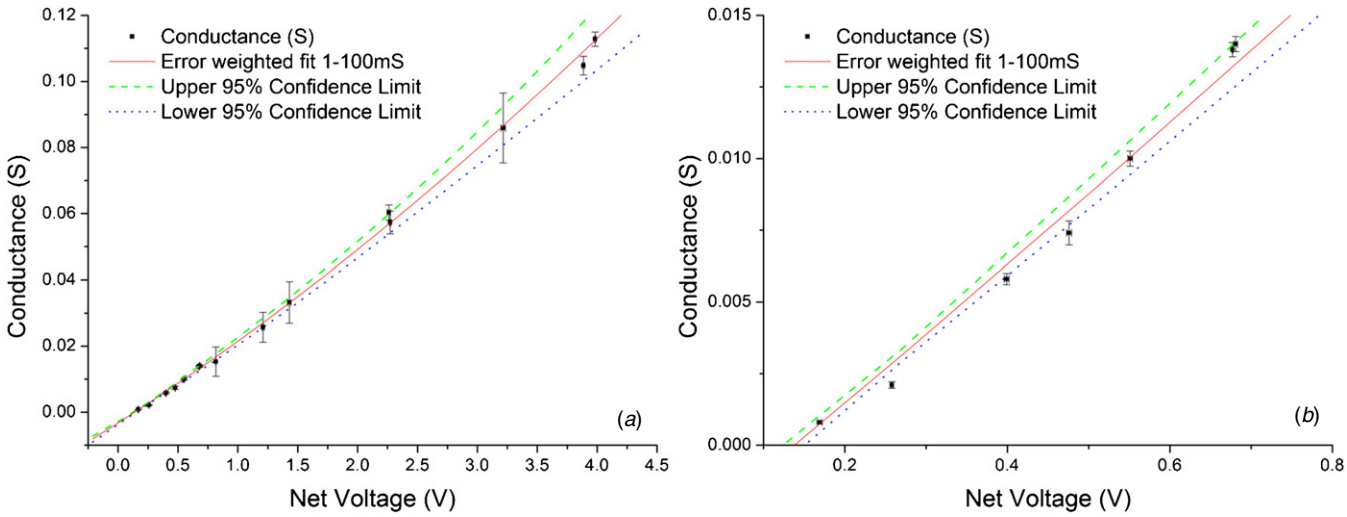

Figure 3. Calibration of a WCT-120 inductive coil across the range (*a*) 1–100 mS and (*b*) 1–15 mS.

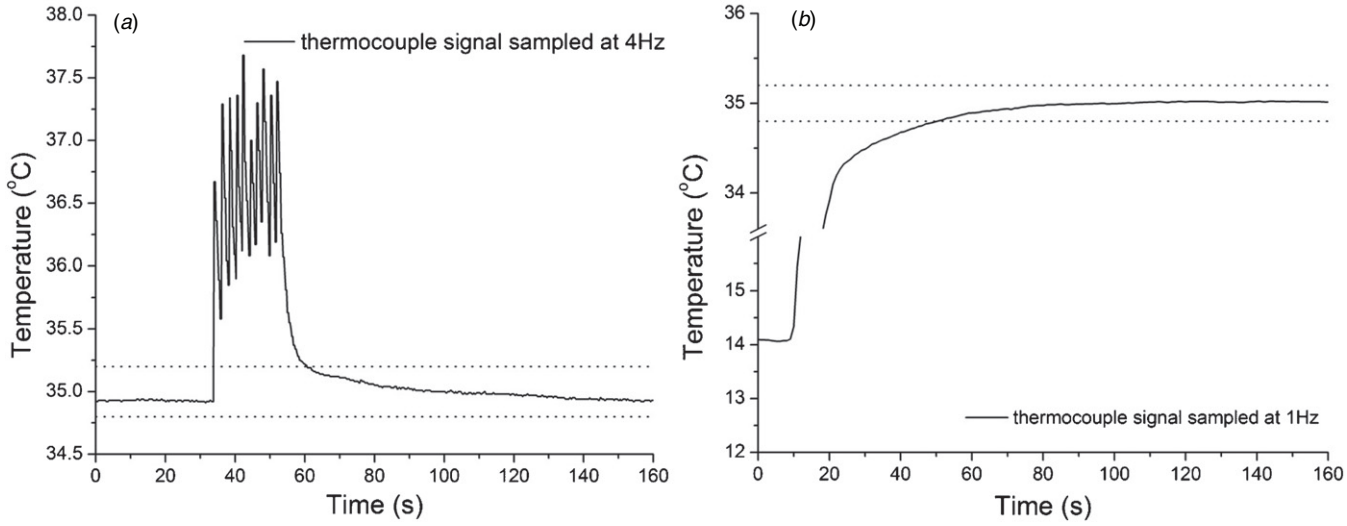

Figure 4. (*a*) Effect of the ten high-intensity flashes used to break Fe_i–B pairs on the sample temperature. (*b*) The time it takes for the sample temperature to equilibrate to the stage temperature once removed from a cold aluminium block. The dotted lines in both figures represent the ±0.2 °C error range.

of the non-diffused samples were four point probe mapped by Solecon.[14]. The diffused samples were four point probed in-house. The impact of the different stage temperatures of the four point probes and the WCT-120 on the conductivity of the wafers was accounted for.

Figure 3 displays the error weighted fit for the conductance range 1–100 mS. To determine the *x*-axis error bars, the samples were repeatedly placed on the coil, their voltage recorded and then removed from the coil. The standard deviation of these voltage data is plotted as the *x*-axis error bars. These error bars are difficult to see as the error was very small. The *y*-axis error bars reflect the standard deviation of the four point probe data.

3.4. The complete randomization of Fe_i

To accurately determine τ_{assoc}, the interstitial Fe population must be randomly distributed through the Si lattice prior to repairing. The impact of incomplete randomization on the resulting repairing curve is shown in figure 2. Two methods were employed to dissociate the Fe_i–B pairs. The first method dissociates the Fe_i–B pairs by flashing the sample ten times with a high-intensity flash (∼500 Suns, 10 ms pulses), while the sample is inside the modified WCT-100, at temperature and ready for data acquisition. The main advantage of method 1 is that one can quickly start acquiring data as the sample is already inside the modified WCT-100, and the temperature of the sample quickly returns to equilibrium (as shown in figure 4(*a*)) after exposure to the flashes. This is useful if the differences between the effective lifetimes of the dissociated and associated states are small, as it maximizes the resolution between the two states. The disadvantage of method 1 is the possibility of incomplete randomization of Fe atoms throughout the silicon lattice. Method 1 was found to be satisfactory for samples with resistivities $<1\ \Omega$ cm.

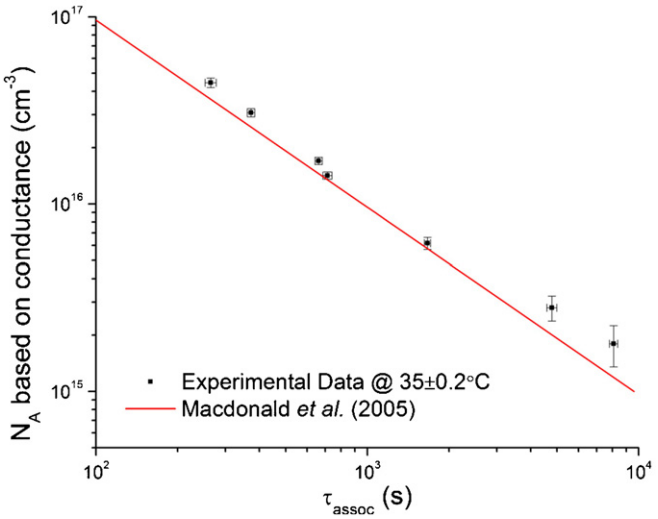

Figure 5. Comparison of new experimental data with the original model.

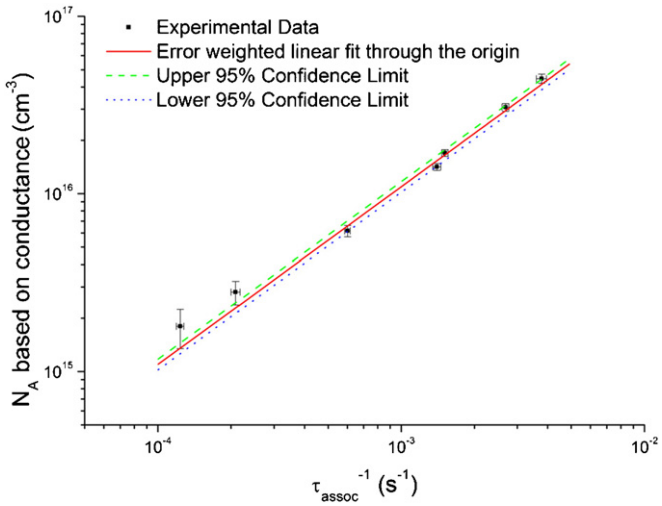

Figure 6. The slope of N_A as a function of inverse τ_{assoc} is proportional to the prefactor.

The second method used to dissociate the Fe_i–B pairs involves exposing the sample to steady-state illumination >200 mW cm^{-2} for 3 min, while the sample sits on a cold block of aluminium. The main advantage of this method is the guarantee of complete randomization of Fe atoms through the silicon lattice. The disadvantage is the inability to take data quickly after dissociation, as the sample must be loaded into the WCT-100 and return to thermal equilibrium (typically ~60 s, as shown in figure 4(*b*)) before data acquisition can begin. Method 2 was found to be necessary for samples with resistivities >1 Ω cm, as in such cases the dopant atoms are further apart, and a greater degree of diffusion of the Fe atoms under illumination is required to fully randomize their distribution.

4. Results and discussion

The same methodology applied by Macdonald *et al* [6] to extract τ_{assoc} from the effective lifetime exponential decay curves has been used in this paper. Figure 5 plots N_A as a function of τ_{assoc}. The *x*-axis error bars are derived from the standard deviation of the τ_{final} measurements. The *y*-axis error bars of figure 5 are based on the 95% confidence limits of the coil calibrations shown in figure 3. The data points plotted in figure 5 do not fit the original Fe_i–B repairing model very well. A new fit is clearly required.

Figure 6 displays the error weighted linear fit through the origin of the inverse τ_{assoc} data versus N_A. The *x*-axis error bars are a combination of the temperature error (±0.2 °C) and the standard deviation of the τ_{final} data. The *y*-axis error bars are based on the 95% confidence limits of the coil calibrations shown in figure 3. Figure 6 differs from the typical plots which link τ_{assoc} and N_A, as the axis have been reversed. There are two good reasons for this. Firstly, the resulting expression will be predominately used to extract N_A by measuring τ_{assoc}. Hence τ_{assoc} is the input. Secondly, the weighted linear regression only accounts for the *y*-axis errors, as the *x*-axis is assumed to be a known input. As the errors associated with τ_{assoc} are consistently between ±2% and 5%, while the errors in N_A vary between ±1.5% and 11%, fitting the regression in this manner accounts for the largest source of uncertainty.

Taking the slope of the fit from figure 6 and accounting for the known parameters give a prefactor of 5.7×10^5 cm^{-3} K^{-1} ±7%. The error in the new prefactor incorporates the temperature error, τ_{final} error and conductance error, and is based on linear fits through the upper and lower 95% confidence limits (±5.4%) shown in figure 6, and the largest *x*-axis error bar (±4.7%). The new expression relating N_A and τ_{assoc} is shown below:

$$N_A = \frac{5.7 \times 10^5}{\tau_{assoc}} T \exp\left(\frac{0.66}{kT}\right)$$

The new prefactor is 14% larger than that determined by Macdonald *et al* (5.0×10^5 cm^{-3} K^{-1} ±3 K). This also indicates that the prefactor for the diffusivity of Fe in silicon (at 35 °C) should decrease from 1.1×10^{-3} [6, 15] to 9.65×10^{-4} cm^2 s^{-1}, as the diffusion of Fe through silicon is the dominant mechanism behind the reformation of the Fe_i–B pairs [6]. For the dopant range tested, ~1×10^{15}–1×10^{17} cm^3, the methodology used in this paper indicates that N_A can be determined within 7% uncertainty. This would correspond to a temperature uncertainty of less than ±1 K, and a paired lifetime standard deviation less than 1%. The new expression has reduced the uncertainty of N_A derived from the repairing rate of Fe_i–B pairs by approximately a factor of 3.

5. Conclusions

Carefully measured and analysed data have allowed a more accurate determination of the pre-factor used in the expression which relates the association time, τ_{assoc}, of Fe_i–B pairs to the acceptor concentration. The new pre-factor determined here (5.7×10^5 cm^{-3} K^{-1}) should allow a more accurate modelling of the formation rate of Fe_i–B pairs. This will benefit special applications of the equation, such as the measurement of boron

concentrations in compensated silicon. The uncertainty of N_A derived from this expression has been reduced from ±24% to ±7%.

Acknowledgment

This work was supported by the Australian Government Department of Innovation, Industry, Science and Research through the International Science Linkages Scheme, Project no CG100017.

References

[1] Macdonald D, Cuevas A and Geerligs L J 2008 Measuring dopant concentrations in compensated p-type crystalline silicon via iron-acceptor pairing *Appl. Phys. Lett.* **92** 202119

[2] Lim B, Liu A, Macdonald D, Bothe K and Schmidt J 2009 Impact of compensation on the deactivation of boron-oxygen recombination-centers in crystalline silicon *Appl. Phys. Lett.* **95** 232109

[3] Peter K, Kopecek R, Wilson M, Lagowski J, Enebakk E, Sioland A and Grandum S 2010 Multicrystalline solar grade silicon solar cells *35th IEEE Photovoltaics Specialists Conf. (HI, USA, 2010)* at press

[4] Geilker J, Kwapil W, Reis I and Rein S 2010 Doping concentration and mobility in compensated material: comparison of different determination methods *Proc. 25th European Photovoltaic and Solar Energy Conf. (Valencia, Spain, 2010)* at press

[5] Tan J, Pascoe A, Macdonald D and Cuevas A 2009 A novel method to determine the majority carrier mobility in p-type multicrystalline silicon *Proc. 24th European Photovoltaic and Solar Energy Conf. (Hamburg, Germany, 2009)* pp 489–51

[6] Macdonald D, Roth T, Deenapanray P N K, Bothe K, Pohl P and Schmidt J 2005 Formation rates of iron-acceptor pairs in crystalline silicon *J. Appl. Phys.* **98** 083509

[7] Paudyal B B, McIntosh K R, Macdonald D H, Richards B S and Sinton R A 2008 The implementation of temperature control to an inductive-coil photoconductance instrument for the range of 0 to 230 °C *Prog. Photovolt., Res. Appl.* **16** 609–13

[8] Klaassen D B M 1992 Unified mobility model for device simulation: II. Temperature dependence of carrier mobility and lifetime *Solid-State Electron.* **35** 961

[9] Klaassen D B M 1992 A unified mobility model for device simulation: I. Model equations and concentration dependence *Solid-State Electron.* **35** 953

[10] Arora N, Hauser J and Roulston D 1982 Electron and hole mobilities in silicon as a function of concentration and temperature *IEEE Trans. Electron Devices* **ED-29** 292–5

[11] Thurber W R, Mattis, Liu Y and Filliben J 1980 Resistivity-dopant density relationship for boron-doped silicon *J. Electrochem. Soc.* **127** 2291–4

[12] http://www.picotech.com/thermocouple.html

[13] http://www.sintoninstruments.com/Sinton-Instruments-WCT-120.html

[14] www.solecon.com

[15] Nakashima H, Sadoh T, Kitagawa H and Hashimoto K 1994 Diffusion and electrical properties of 3d transition-metal impurity series in silicon *Mater. Sci. Forum* **143–147** 76